STRATEGIES FOR REDUCTING PEAK DEMAND IN NET-ZERO ENERGY SOLAR HOMES

José A. Candanedo[1] and Andreas K. Athienitis[1]

[1]BCEE Department, Concordia University, Montreal (Canada)

1. Introduction

This paper investigates strategies to reduce peak loads in net-zero energy solar homes through the coordination of different design and operation strategies. The concept of net-zero energy homes, roughly defined as grid-tied houses that supply their energy needs with renewable energy sources over a period of interest, has gained in popularity in recent year. In spite of the clear advantages of this design approach, it is necessary to address the issue of peak loads and their impact on utility grids. Even if the net-zero energy goal is achieved during the period of assessment (e.g., one year), significant imbalances may be observed at smaller time scales. For instance, in northern latitudes, the generation of PV panels typically exceeds the energy use of the house during the summer months, while in winter the energy use of the house is larger than the generation of the PV system. Fluctuations of the ratio generation/use are also registered during the daily cycle. If a net zero energy house draws energy from the utility grid during peak periods, its impact on the grid will be similar to that of a conventional home, with the subsequent need for increased generation and transmission capacity.

It is well known that the net-zero energy goal can be achieved through the use of passive solar design techniques and active solar technologies. However, opportunities to improve the interaction of the building with the grid, through a combination of technologies and control strategies, is investigated less often. Some of these strategies are:

- advanced control (model-based predictive control, optimal control)
- energy storage (building's thermal mass, thermal energy storage devices, batteries)
- dynamic fenestration and motorized blinds to regulate solar gains
- information exchange with the grid (smart meters/smart grids)
- demand response (DR) applied to domestic appliances
- energy dashboards to improve communication with the occupants

For example, the thermal mass of the building can be used as an energy storage device by allowing moderate temperature fluctuations without compromising thermal comfort. Night cooling strategies could reduce cooling needs the following day. Conversely, during winter, passive solar gains collected during the daytime may reduce the need for heating at night: such a strategy has the potential of reducing peak loads significantly in places where electricity is used for heating.

This paper presents the results of simulation studies designed to evaluate different peak load reduction strategies for net-zero energy solar homes. Scenarios based on different weather pattern sequences in a cold climate will be applied.

2. Model Predictive Control

Model predictive control (MPC) is the generic name given to a set of advanced control techniques that use load and weather forecasts, as a well as a model of the building, in order to improve the operation of the system (Fig. 1). MPC usually implies applying an optimization algorithm to reduce a "cost" function subject to a set of constraints (Gyalistras, 2010). In the case of a building, the cost function is typically the energy price, total energy use or peak loads. Common constraints are thermal comfort or maximum rating of the HVAC equipment.

MPC strategies, which may be applied at the supervisory and local-loop control levels, can be used to manage the energy storage capabilities of the building, either thermal or electrical. Peak load reduction implies managing the collection, storage and delivery of renewable energy resources. Energy storage devices

are essential to accomplish this task. Also, measures that permit regulating the entry of solar gains into the building may be used to use them more effectively to satisfy heating needs while preventing discomfort due to overheating or glare.

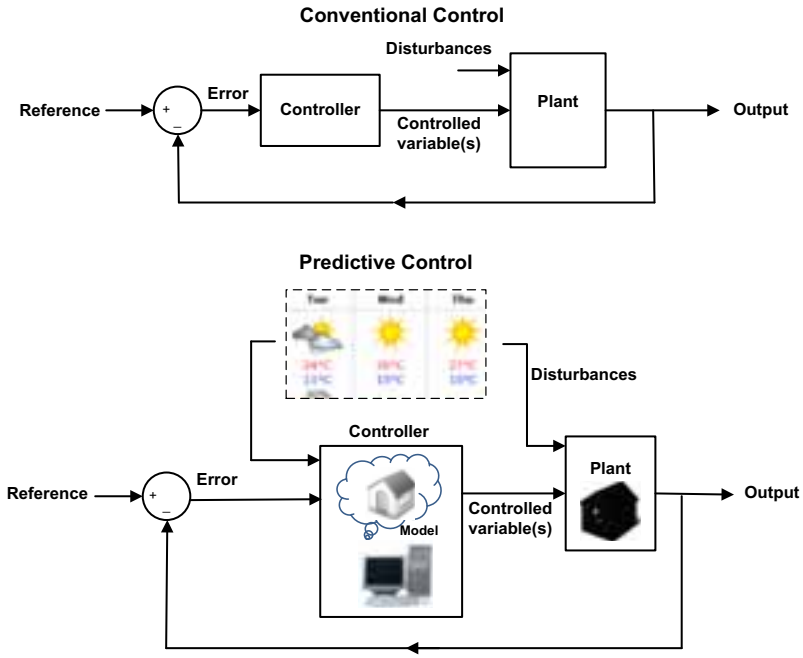

Fig. 1: Conventional control (above) versus Model Predictive Control.

Although the idea of applying MPC for buildings has been investigated since the 1980s (Vinot, 1988; Paassen, 1989; Nygård-Ferguson and Scartezzini, 1989), it is receiving increasing attention in recent years, because of increased awareness on environmental issues, faster and smaller processors and the widespread availability of online weather forecasts. Henze et al. (2005), Braun (2003) and collaborators have investigated the application of predictive control, mainly in commercial buildings. Kummert (1996) studied the application of predictive control to solar buildings with a simplified model. Recently, Kummert's investigations on predictive control have been extended to commercial buildings (Kummert, 2005). Ma et al. (2010) and Gyalistras (2010) –among numerous other researchers– have recently added relevant work to the literature on predictive control applied to buildings.

3. Modeling of a Case Study

An essential problem in the application of MPC is the development of the model itself. This model has to be accurate enough to be a reliable representation of the building; however, it also has to be simple enough to be manageable by the optimization routines of the controller. Selecting the right level of complexity is no easy task, as it involves adopting simplifying assumptions and deciding which inputs can be safely neglected.

A pathway to develop a simple yet dependable model consists in the application of system identification techniques. With this method, data obtained from measurements or from the result of a detailed building simulation can be used to create a model (Candanedo and Athienitis, 2010; Candanedo et al. 2011).

To illustrate the application of this principle, a case study loosely based on an actual near net-zero energy solar house, the EcoTerra House, in Québec, Canada (Chen et al., 2010) is presented. The case study consists of a building of approximately 230 m^2, with a rectangular cross-section and walls oriented towards the cardinal directions. The with wall insulation of R-34 (U_W = 0.16.7 W/m^2/K). Triple glazed, low emissivity windows cover 40% of the south façade. A radiant floor heating (RFH) system is installed in a concrete floor 5 cm (2-in) thick. The radiant floor heating is assumed to be installed 1.25 cm from the bottom of the floor (3.75 cm below the surface). Infiltration is fixed at 0.25 air changes per hour. This building is modeled by using a 6-node thermal network model adapted from the model presented in (Athienitis, 1994). The

calculation of the solar gains takes into account the variation of incidence angles due to the sun's position. About 70% of the solar gains are received by the surface of the floor, while the other 30% is distributed evenly in the remaining internal surfaces.

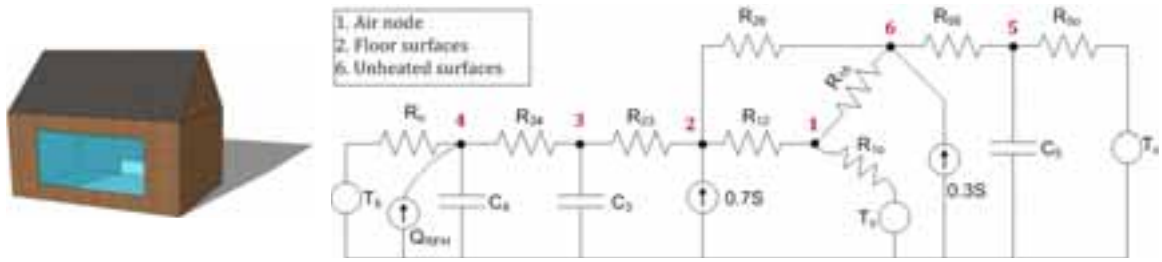

Fig. 2: Case study building. Thermal network model used for the case study building.

For the purpose of the control strategy, a simplified transfer function model was developed (Fig. 3). This model consists of a set of three transfer functions. The transfer function model, based on the assumption of linearity, is obtained by observing that (in this particular case of a well-insulated, air-tight building with large windows) the dominant inputs in the building are solar gains, outdoor temperature, and heat from the RFH system. Other variables that have a smaller impact on the thermal response of the building (e.g., wind speed, humidity) are neglected.

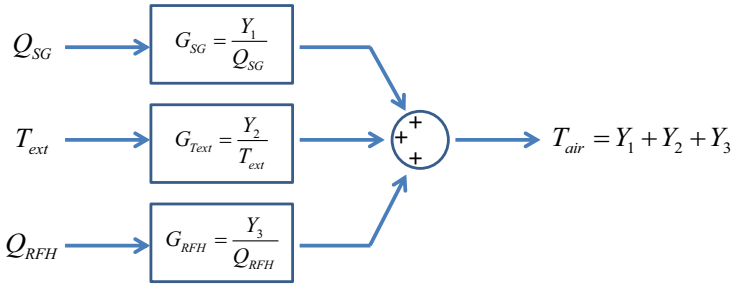

Fig. 3: Transfer function model used to model the building.

The transfer functions are found by carrying out "numerical experiments" on the system (Candanedo et al. 2011). Forcing functions, consisting of repeating patterns of solar radiation, outdoor temperature and RFH heat, are applied to the system. Each response is studied independently (for example, the response to outdoor temperature is found while keeping the solar radiation values at zero) and then the total response can be found by superposition (Candanedo and Athienitis, 2010). The transfer functions are found with MATLAB's System Identification Toolbox (Ljung, 1999; Ljung, 2010). Although it is not strictly necessary to find the response to each input independently, such an approach facilitates comparing their relative impact and provides insight on the building.

Transfer functions have been used for energy simulation in buildings since the 1960s (Mitalas and Stephenson, 1967), either for entire rooms or for building components. Conduction transfer factors (CTFs) are widely used to treat conduction through walls, floors and ceilings in tools such as EnergyPlus and TRNSYS. They are the basis of ASHRAE's heat balance method (Rees et al., 2000). Transfer functions used in ASHRAE's load calculation or in building simulation are determined with analytical methods based on properties of the materials and construction details. In contrast, the methodology discussed in this paper follows a "reverse approach": transfer functions intended for control purposes are found by using building simulation results or measurements as the starting point.

Figures 4, 5 and 6 show respectively the response of the indoor air temperature to "forcing functions" for solar gains, outdoor temperature and RFH input.

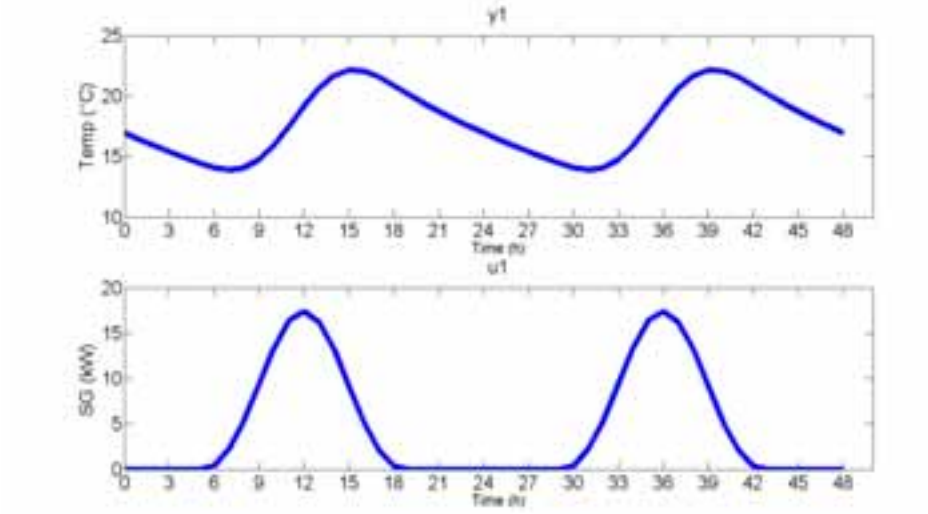

Fig. 4: Response of the indoor air temperature to solar gains.

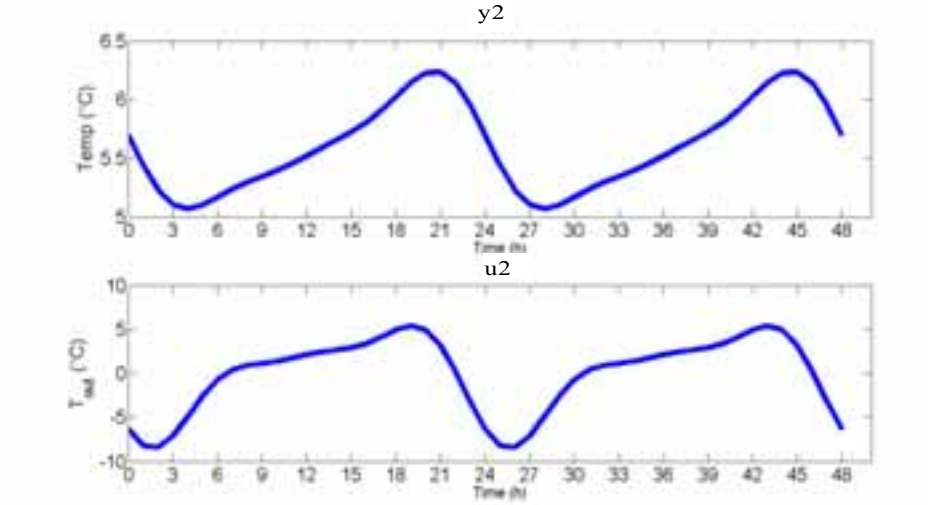

Fig. 5: Response of the indoor air temperature to outdoor temperature.

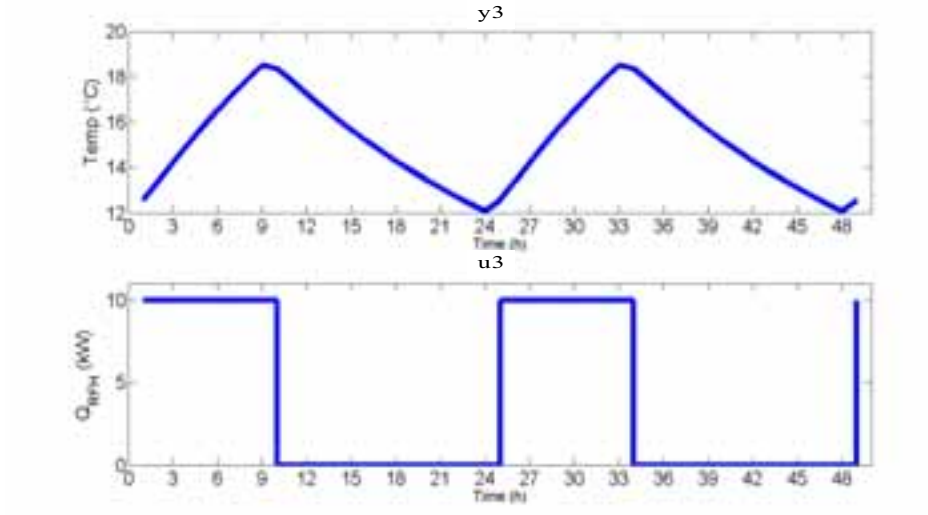

Fig. 6: Response of the indoor air temperature to the radiant floor heating system.

The relationship between inputs and outputs is given by *time series* model in this case. A time series representation is equivalent to z-transform transfer function. The model presented here is an autoregressive moving average model with exogenous input (ARMAX), in which the word autoregressive means that the current output, $y(t)$, is correlated with its own previous values, while the "exogenous input" refers simply to the input variable(s) $u_i(t)$. It is given by (Ljung 2010):

$$A(q)y(t) = \sum_{i=1}^{nu} B_i(q)u_i(t - nk_i) + C(q)e(t) \qquad \text{(eq. 1)}$$

in which in which $A(q)$, $B(q)$ and $C(q)$ are polynomials in terms of q^{-1}; this is the "backward-shift operator", equivalent to the z^{-1} in a z-transform, $y(t)$ is the sequence of output values, $u_i(t)$ is the input sequence i, nu is the number of inputs, and $e(t)$ is a sequence of noise values. For a single input (nu = 1), (eq. 1) becomes:

$$A(q)y(t) = B(q)u(t - nk) + C(q)e(t) \qquad \text{(eq. 2)}$$

The transfer function between the output $y(t)$ and the input $u(t)$ is then given by:

$$G(q) = \frac{y(t)}{u(t)} = \frac{B(q)}{A(q)} \qquad \text{(eq. 3)}$$

The models were found with the SI toolbox for the three transfer functions presented above, namely solar gains, outdoor temperature and RFH input. These models, obtained for one-hour intervals, are given by:

$$\frac{y_1(t)}{u_1(t)} = \frac{0.1253 - 0.05021q^{-1}}{1 - 1.388q^{-1} + 0.4072q^{-2}} \quad \left[\frac{°C}{kW}\right] \qquad \text{(eq. 4)}$$

$$\frac{y_2(t)}{u_2(t)} = \frac{0.0427 - 0.03286q^{-1}}{1 - 1.461q^{-1} + 0.4606q^{-2}} \quad \left[\frac{°C}{°C}\right] \qquad \text{(eq. 5)}$$

$$\frac{y_3(t)}{u_3(t)} = \frac{0.08041 + 0.02845q^{-1}}{1 - 1.065q^{-1} + 0.09194q^{-2}} \quad \left[\frac{°C}{kW}\right] \qquad \text{(eq. 6)}$$

To illustrate how these transfer functions can be used to model the system, through some algebraic manipulation (eq. 4) becomes:

$$y_1(t) = 1.388y(t - \Delta t) - 0.4072y(t - 2\Delta t) + 0.1253u_1(t) - 0.05021u_1(t - \Delta t) \qquad \text{(eq. 7)}$$

This means that the current value of the output, $y_1(t)$, depends on previous output values "one hour ago" (Δt) and "two hours ago" (2Δt). It also depends on the input's current value $u_1(_t)$ and "one hour ago" (Δt).

4. Simulation of Control Strategies

With the transfer function model presented above, and some information on future weather, it is possible to calculate the amount of heat that the RFH needs to deliver to follow the set-point, or at least to minimize the discrepancies between the set-point and the actual temperature obtained. The problem then consists of determining the optimal set-point trajectory for a given objective function and tracking the desired set-point as accurately as possible (or at least, without any comfort complains).

4.1 Predictive control for set-point tracking

Let us assume that, at a midnight during winter, the weather forecast indicates that the solar gains and the outdoor temperatures are given by the curves shown below (Fig. 7):

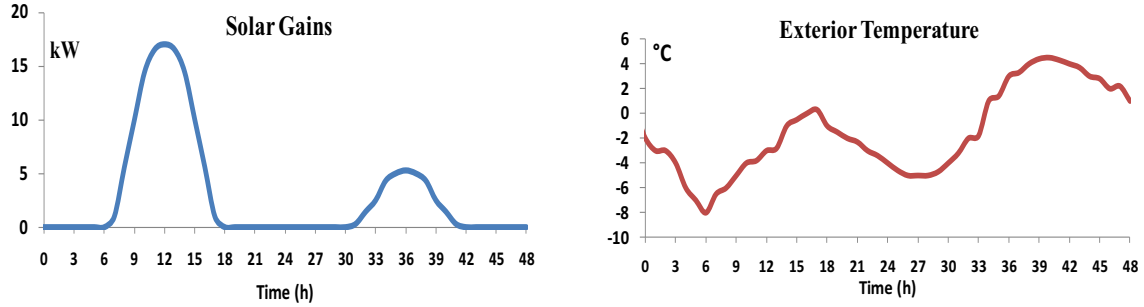

Fig. 7: Input variables from the weather forecast for a 48 hour period.

The problem will then consist of determining the optimal heating rated delivered by the radiant floor heating system to satisfy the set-point. An alternative for the objective function can be:

$$J = \sqrt{\sum_{i=1}^{n} \left(T_{sp,i} - T_{air,i} \right)^2} \qquad \text{(eq. 8)}$$

In this case the objective function J is equal to the norm of the error (i.e., difference between the set-point and the temperature measured). The solution is subject to the constraint shown below, which accounts for the absence of cooling equipment:

$$Q_{RFH,i} > 0; \qquad \text{(eq. 9)}$$

For example, let us assume that a fixed set-point value of 21 °C is used for the entire 48-hr period. If the initial temperature conditions have been 21 °C for a couple of hours, and the effect of white noise is ignored the free floating response (i.e., without the intervention of the heating system) is given by the curve shown to the left of Fig. 8. Although software tools exist for the implementation of MPC (Bemporad et al., 2010) which have been used by the authors of this paper in previous investigations, simple optimization algorithms from MATLAB may also be used to obtain the heating curve. Both the heating curve and the temperature response are shown in Fig. 8.

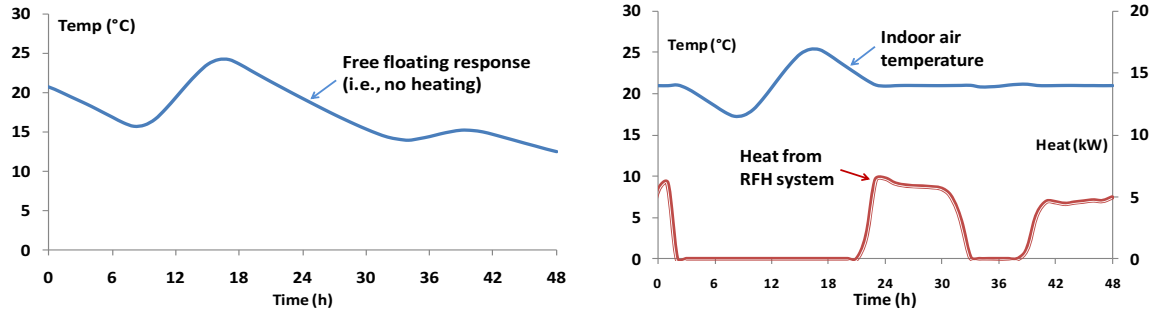

Fig. 8: Free floating response (left); response with optimal heating to approach a fixed 21 °C set-point (right).

It is evident that it is not possible to keep the temperature at 21 °C without cooling. However, the temperature rise over 25 °C may be acceptable. It is also interesting that the heating system remains off for relatively long periods. The maximum heating rate is 6.5 kW before midnight of the second day. It is worth mentioning that the optimization is significantly facilitated by using a simple transfer function model.

4.2 A more complex objective function

The objective function can take different forms. It can be total energy, peak load or cost; it may also be a composite of factors, each of which receives a certain weight. The cost function can include several different elements into the "accounting": for example, heating/cooling, lighting, appliances, fans and pumps. The comfort aspect may also be introduced as a constraint, or as another "weighted factor".

In the example presented here, the cost function will be a combination of economic cost (which can often account for the impact of peak loads) and comfort. Although TOU rates are not used at the residential level in Québec, a hypothetical curve selected is based on the fact that residential peak loads tend to occur in the morning (roughly between 6:00 and 8:00) and in the evening (17:00 to 21:00). The time-of-use (TOU) selected is given by the following function (Fig. 9):

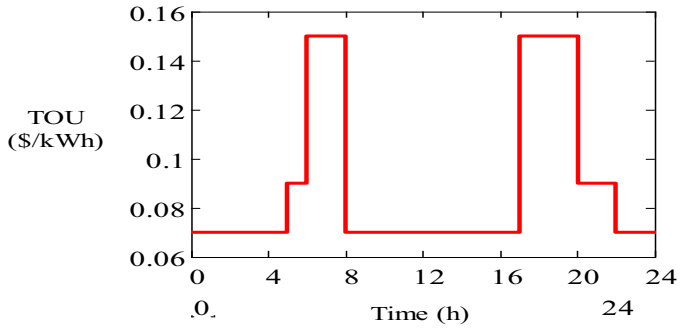

Fig. 9: TOU rate ($/kWh) used in this case study.

The objective function used in this example is given by:

$$J = \alpha \int_{0}^{Period} TOU(t) * Q_{RFH}(t)dt + (1-\alpha)\left\{\sqrt{\sum_{i=1}^{n}\left(T_{sp,i} - T_{air,i}\right)^2}\right\} + \gamma D \qquad \text{(eq. 10)}$$

in which α is weighting factors between 0 and 1. This variable does not have an intrinsic physical meaning; rather, it works as an "adjusting knob" to change the relative importance of economic cost or comfort. The factor γ is a large number (10^8) that has been introduced to prevent extreme discomfort situations; the variable D is equal to 1 if the temperature exceeds 30 °C or falls below 17 °C.

When α = 0.3, the optimization routine yields the results shown in Fig. 10:

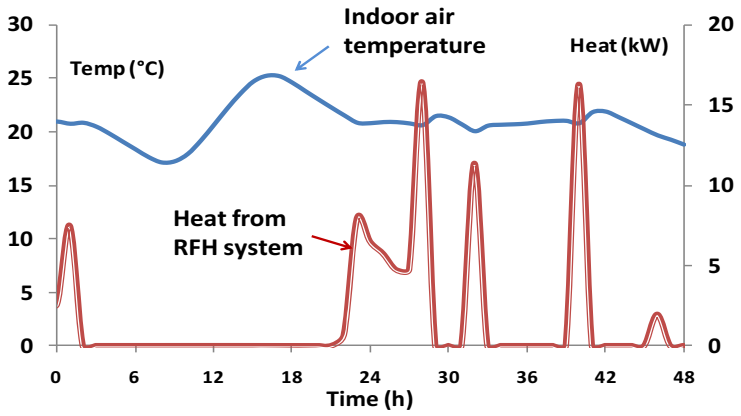

Fig. 10: Optimization results for α = 0.3. No bounds set for peak load.

In this case, the total economic cost for the 48 hr is $6.34. The heating system practically does not work during the morning and evening, but there are large peaks at night and in the middle of the day. In this case, the limitation might actually be the rated power of the heating system. By running the optimization with a maximum heating value set to 10 kW, the following results are obtained (Fig. 11):

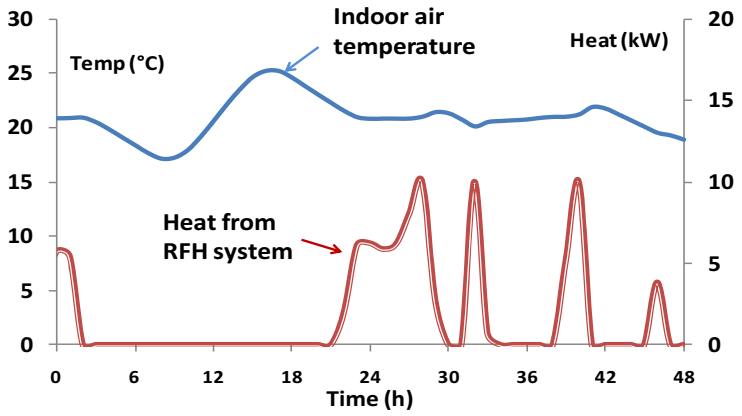

Fig. 11: Optimization results for $\alpha = 0.3$ and maximum heating output set at 10 kW.

In this case the peak heating power is limited, but the indoor air temperature results are not perceptibly affected. Although a 10 kW peak is higher than that presented in Fig. 8 (equivalent to $\alpha = 0$), it is important to recall that the impact of peak loads depends on their *time* of occurrence. Larger peaks at the residential level may be better handled by the utility if they occur during the off-peak hours of the grid.

Figure 12 shows the results when $\alpha = 0.3$ (i.e. more importance given to cost).

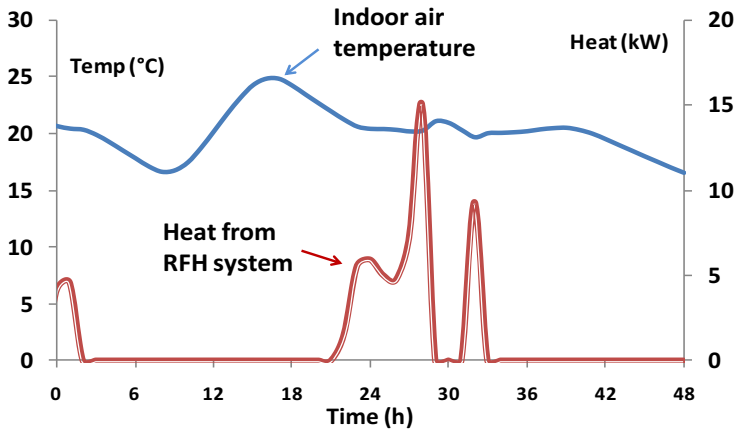

Fig. 12: Optimization results for $\alpha = 0.7$. No bounds set for peak load.

In this case, the optimization yields a peak load of 14.98 kW, for a total cost of $4.41. Thermal comfort problems start to appear at the end of the period. Finally, Fig. 13 shows the results obtained when the heating output is limited to 10 kW.

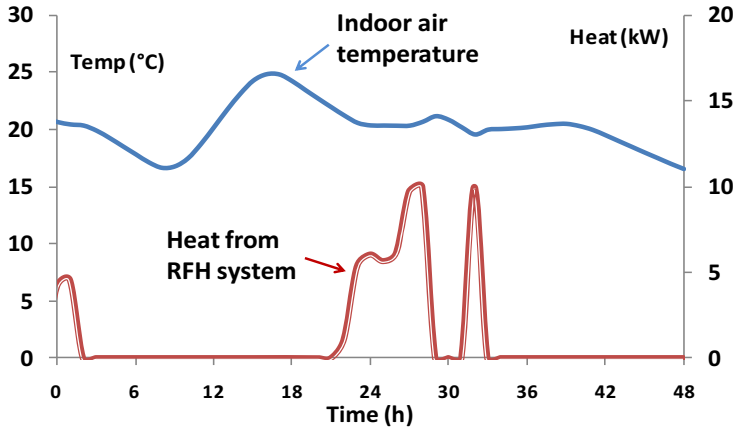

Fig. 13: Optimization results for $\alpha = 0.7$. Upper bound for peak load at 10 kW.

4.3 Solar gains control

To illustrate the importance of solar gains control, let us assume that the expected temperature is somewhat warmer (+5°C) and the solar gains are 20% higher. The new input variables are shown in Fig. 14:

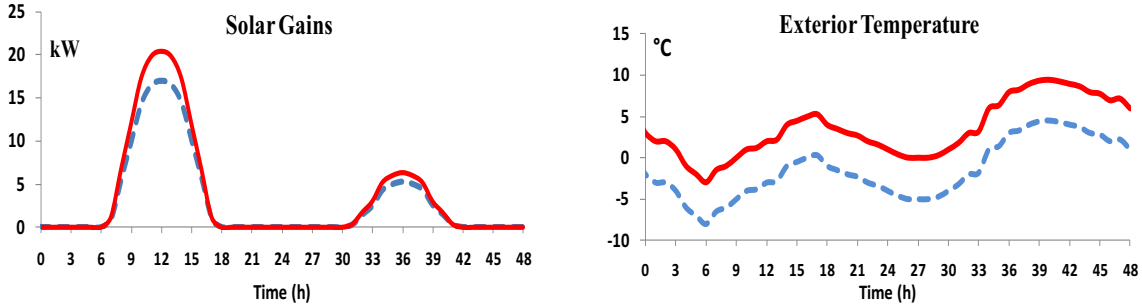

Fig. 14: Modified input variables to investigate overheating prevention.

With these input variables, and a value of $\alpha = 0.5$, the optimization algorithm yields the results shown in Fig. 15. Although the heating system only operates during a brief period, there is a significant temperature fluctuation during the first day. The maximum temperature value exceeds 28 °C; such conditions might produce discomfort.

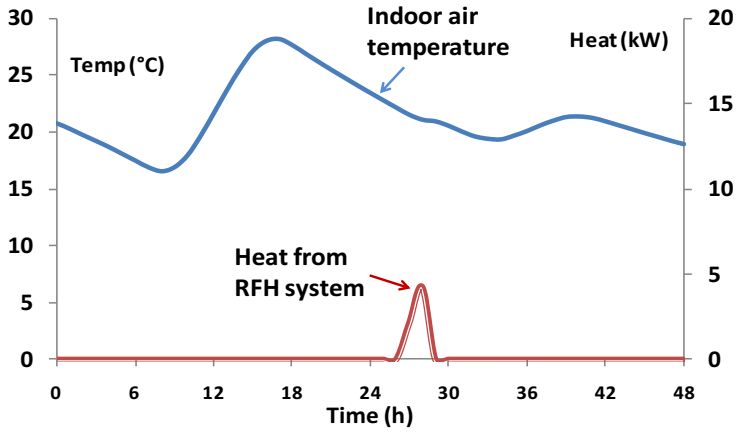

Fig. 15: Response of optimization algorithm with modified input values.

In order to avoid such a large temperature fluctuation, a roller blind, a venetian blind, an electro-chromic window or another dynamic fenestration device could be used to reject excessive solar gains. Assuming that such a device allows rejecting 35% of the solar gains during the first day (i.e. effective transmittance $\tau = 0.65$), the optimization algorithm is used again to calculate the response of the system.

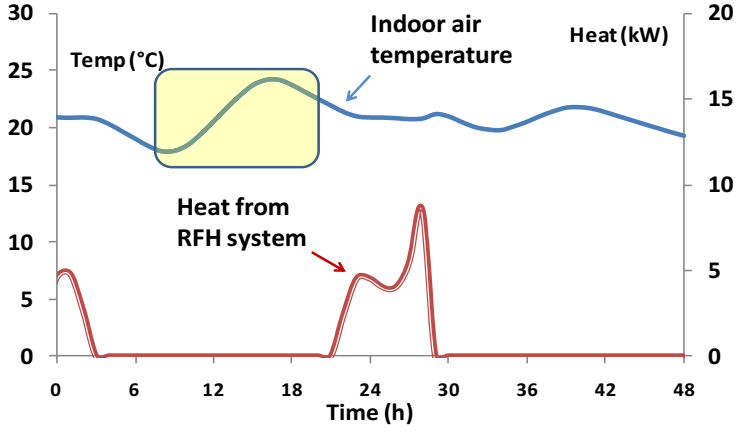

Fig. 16: Reduced temperature fluctuation through predictive control of solar gains.

The regulation of solar heat gains reduces the temperature fluctuation on the first day; however, as expected, since less heat is accumulated in the building structure, the RFH system has to release more thermal energy in order to maintain comfort.

5. Discussion and Conclusions

Predictive control is among the strategies that can be used to reduce peak loads in solar homes. Other technologies or strategies which can be used as a complement of predictive control include solar gains regulation, energy storage devices and economic incentives. The use of a simplified building model eases the implementation of predictive control; such an implementation can be challenging (though not impossible) in a detailed building simulation tool for real time control. As expected, different objective functions have a significant impact in the results obtained with the optimization.

Future investigations will make use of load matching and grid interaction indicators to evaluate the impact of different control strategies (Verbruggen et al. 2011; Salom et al. 2011), both from the point of the view of the building owner and from the point of view of the utility grid.

6. Acknowledgements

The work presented in this paper has largely been developed in the context of the International Energy Agency (IEA) joint programme: Solar Heating and Cooling (SHC) Task40 and Energy Conservation in Buildings and Community Systems (ECBCS) Annex52: Towards Net Zero Energy Solar Buildings. The authors would like to acknowledge the financial support of the Canadian National Science and Engineering Research Council through the strategic Solar Buildings Research Network.

7. References

Athienitis, A.K. 1994. Building Thermal Analysis. Electronic Book Mathcad, MathSoft, Boston, USA.

Bemporad, A., Morari, M., Ricker, N.L. 2010. Model Predictive Control Toolbox 3 User's Guide. The Mathworks.

Braun, J.E. (2003). Load Control Using Building Thermal Mass. Journal of Solar Energy Engineering 125, 292.

Candanedo, J.A., Allard, A., Athienitis, A.K., 2011, Predictive control of radiant floor heating and transmitted irradiance in a room with high solar gains, ASHRAE Transactions, 117(2).

Candanedo, J.A., Athienitis, A.K., 2011, Predictive control of radiant floor heating and solar-source heat pump operation in a solar house, HVAC & R Research 17 (3): 235-256 , June 2011.

Chen, Y., Athienitis, A.K., Galal, K. 2010. Modeling, design and thermal performance of a BIPV/T system thermally coupled with a ventilated concrete slab in a low energy solar house: Part 1, BIPV/T system and house energy concept. Solar Energy 84(11), 1892-1907.

Gyalistras, D., OptiControlTeam. 2010. Final Report: Use of Weather and Occupancy Forecasts for Optimal Building Climate Control (OptiControl). Report: ETH Zürich. Zürich, Switzerland.

Henze, G.P., Kalz, D.E., Liu, S., Felsmann, C. (2005). Experimental analysis of model-based predictive optimal control for active and passive building thermal storage inventory. HVAC & R Research 11(2), 189-213.

Kummert, M., André, P., Nicolas, J. 1996. Development of simplified models for solar buildings optimal control. In Proceedings of ISES Eurosun 96 Congress, 1055-1061., Freiburg, Germany. September 16-19.

Kummert, M., André, P. 2005. Simulation of a Model-Based Optimal Controller for Heating Systems under Realistic Hypothesis. In Ninth International IBPSA Conference, Montréal, Canada.

Ljung, L. 1999. System Identification: Theory for the User. Second Edition. Prentice Hall, Upper Saddle River, New Jersey.

Ljung, L. 2010. System Identification Toolbox™-7: User's Guide - MATLAB & Simulink. The Mathworks, Inc., Natick, MA. URL: http://www.mathworks.com/help/pdf_doc/ident/ident.pdf

Ma, Y., Borrelli, F., Hencey, B., Coffey, B., Bengea, S., Haves, P. (2010). Model Predictive Control for the Operation of Building Cooling Systems. In American Control Conference, Baltimore, Maryland, USA. June 30-July 2.

Mitalas, G., Stephenson, D. 1967. Room thermal response factors. ASHRAE Transactions 73(1), 1-15.

Nygård-Ferguson, M., Scartezzini, J.-L. 1989. Computer simulation of an optimal stochastic controller applied to passive solar rooms. Energy & Buildings 14, 1-7.

Paassen, A.H.C.v. 1989. Passive Building Control. In CLIMA 2000 II. Heating Components and Systems, Sarajevo, Yugoslavia. August 27-September 1.

Rees, S., Spitler, J., Davies, M., Haves, P. 2000. Qualitative comparison of North American and UK cooling load calculation methods. International Journal of Heating, Ventilating, Air-Conditioning and Refrigeration Research 6(1), 75-99.

Salom, J., Widén, J., Candanedo, J., Sartori, I., Voss, K., Marszal, A. 2011. Understanding net-zero energy buildings: evaluation of load matching and grid interaction indicators. In Twelfth International IBPSA Conference, Sydney, Australia, November 14-16.

Verbruggen, B., Coninck, R.D., Baetens, R., Saelens, D., Helsen, L., Driesen, J., 2011. Grid impact indicators for active building simulation. In IEEE PES Conference on Innovative Smart Grid Technologies, Anaheim, California, January 17-19.

Vinot, B. 1988. Combined Control of Direct Gains and Heating in Passive Solar Buildings. In PLEA88 - Energy and Buildings for Temperate Climates: a Mediterranean Regional Approach, 583-588, Porto, Portugal. July 27-31.

Nomenclature

$A(q)$, B(q), $C(q)$	Polynomials in terms of the q^{-1} operator
C_i	Thermal capacitance [J/K]
D	Variable to penalize thermal discomfort
$e(t)$	Error signal
J	Objective function
n	Number of time steps
Q_{RFH}	Heat released by radiant floor heating system [W]
Q_{SG}, S	Solar gains [W]
R_{ij}	Resistance between nodes i and j [K/W]
T_{ext}	Outdoor temperature [°C]
T_{air}	Indoor air temperature [°C]
$T_{air,i}$	Air temperature at time step i
$T_{sp,i}$	Set-point temperature at time step i
u_1, u_2, u_3	Inputs of the transfer function system
y_1, y_2, y_3	Individual contributions to output from each input
TOU	Time of use rate ($/kWh)
α	Weighting factor
γ	Factor to penalize discomfort
Δt	Time step
τ	Adjustable transmittance